

Chiral phase transition at high temperature and density in the QCD-like theory

O. Kiriya^{*}, M. Maruyama and F. Takagi

Department of Physics, Tohoku University, Sendai 980-8578, Japan

The chiral phase transition at finite temperature T and/or chemical potential μ is studied using the QCD-like theory with a variational approach. The “QCD-like theory” means the improved ladder approximation with an infrared cutoff in terms of a modified running coupling. The form of Cornwall–Jackiw–Tomboulis effective potential is modified by the use of the Schwinger–Dyson equation for generally nonzero current quark mass. We then calculate the effective potential at finite T and/or μ and investigate the phase structure in the chiral limit. We have a second-order phase transition at $T_c = 129$ MeV for $\mu = 0$ and a first-order one at $\mu_c = 422$ MeV for $T = 0$. A tricritical point in the T - μ plane is found at $T = 107$ MeV, $\mu = 210$ MeV. The position is close to that of the random matrix model and some version of the Nambu–Jona-Lasinio model.

PACS number(s): 11.10.Wx, 11.15.Tk, 11.30.Rd, 12.38.Lg

I. INTRODUCTION

At zero temperature and zero (baryon number) density, the chiral symmetry in quantum chromodynamics (QCD) is dynamically broken. It is generally believed that at sufficiently high temperature and/or density the QCD vacuum undergoes a phase transition into a chirally symmetric phase. This chiral phase transition plays an important role in the physics of neutron stars and the early universe and it may be realized in heavy-ion collisions. At finite temperature the lattice simulation is powerful to study the chiral phase transition at finite temperature ($T \neq 0$). It is now developing also for finite chemical potential ($\mu \neq 0$). However, effective theories of QCD are still useful for various nonperturbative phenomena including the phase transition.

Recently, it has been argued that importance of a study of the phase structure, especially a position of the tricritical point, has been pointed out in Ref. [1]. The Nambu–Jona-Lasinio (NJL) model [2] in which the interaction is induced by instantons and the random matrix model [3] have shown almost the same results concerning the tricritical point. It is also interesting to study the possibility of color superconducting phase at high baryon density [2,4–8]. In this paper, we concentrate on the chiral phase transition between $SU(N_f)_L \times SU(N_f)_R$ and $SU(N_f)_{L+R}$ using the effective potential and the QCD-like theory. One usually studies the phase structure of QCD in terms of the Schwinger–Dyson equation (SDE) or the effective potential [9–13]. However, the use of the SDE only is not sufficient for its study in particular when there is a first order phase transition; then, we use the effective potential. The QCD-like theory provided with the effective potential for composite operators and the renormalization group is successful to study the chiral symmetry breaking in QCD [14,15]. This type of theory is occasionally called *QCD in the improved ladder approximation*. The phase diagram in the QCD-like theory has been studied in Refs. [9,11,13]. However, the position of the tricritical point is largely different from that obtained from the NJL model and the random matrix model.

In this paper we use a modified form of the Cornwall–Jackiw–Tomboulis (CJT) effective potential [16] which is convenient for a variational approach. The formulation is given for the case where the chiral symmetry is explicitly broken at zero temperature and density. We, then, consider the CJT effective potential in the improved ladder approximation at finite temperature and/or density. Being motivated by Refs. [2,3], we re-examine the chiral phase transition and phase structure in the chiral limit.

This paper is organized as follows. In Sec. II we formulate the effective potential for composite operators and extend it to finite temperature and density. In Sec. III we first determine the value of Λ_{QCD} by a condition $f_\pi = 93$ MeV at $T = \mu = 0$ and then calculate the effective potential at finite T and/or μ numerically. Using those results, we study the phase structure in the T - μ plain. Sec. IV is devoted to conclusion. We fix the mass scale by the condition $\Lambda_{\text{QCD}} = 1$, except for Sec. III.

^{*}Email address: kiriya@nucl.phys.tohoku.ac.jp

II. EFFECTIVE POTENTIAL FOR QUARK PROPAGATOR

A. CJT effective potential at zero temperature and density

At zero temperature and zero density, the CJT effective potential for QCD in the improved ladder approximation is expressed as a functional of $S(p)$ the quark full propagator [17]:

$$V[S] = V_1[S] + V_2[S], \quad (1)$$

$$V_1[S] = \int \frac{d^4 p}{(2\pi)^4 i} \text{Tr} [\ln(S_0^{-1}(p)S(p)) - S_0^{-1}(p)S(p) + 1], \quad (2)$$

$$V_2[S] = -\frac{i}{2}C_2 \int \int \frac{d^4 p}{(2\pi)^4 i} \frac{d^4 q}{(2\pi)^4 i} \bar{g}^2(p, q) \text{Tr} (\gamma_\mu S(p) \gamma_\nu S(q)) D^{\mu\nu}(p - q), \quad (3)$$

where $C_2 = (N_c^2 - 1)/(2N_c)$ is the quadratic Casimir operator for color $SU(N_c)$ group, $S_0(p)$ is the bare quark propagator, $\bar{g}^2(p, q)$ is the running coupling of one-loop order, $D^{\mu\nu}(p)$ is the gluon propagator (which is diagonal in the color space) and “Tr” refers to Dirac, flavor and color matrices. The two-loop potential V_2 is given by the vacuum graph of the fermion one-loop diagram with one gluon exchange (see Fig. 1).

After Wick rotation, we use the following approximation according to Higashijima [17] and Miransky [18]

$$\bar{g}^2(p_E, q_E) = \theta(p_E - q_E) \bar{g}^2(p_E) + \theta(q_E - p_E) \bar{g}^2(q_E). \quad (4)$$

In this approximation and in the Landau gauge, no renormalization of the quark wave function is required [19] and the CJT effective potential is expressed in terms of $\Sigma(p_E)$ the dynamical mass function of quark:

$$V[\Sigma(p_E)] = V_1[\Sigma(p_E)] + V_2[\Sigma(p_E)], \quad (5)$$

$$V_1[\Sigma(p_E)] = -2 \int^\Lambda \frac{d^4 p_E}{(2\pi)^4} \ln \frac{\Sigma^2(p_E) + p_E^2}{m^2(\Lambda) + p_E^2} + 4 \int^\Lambda \frac{d^4 p_E}{(2\pi)^4} \frac{\Sigma(p_E)(\Sigma(p_E) - m(\Lambda))}{\Sigma^2(p_E) + p_E^2}, \quad (6)$$

$$V_2[\Sigma(p_E)] = -6C_2 \int^\Lambda \int^\Lambda \frac{d^4 p_E}{(2\pi)^4} \frac{d^4 q_E}{(2\pi)^4} \frac{\bar{g}^2(p_E, q_E)}{(p_E - q_E)^2} \times \frac{\Sigma(p_E)}{\Sigma^2(p_E) + p_E^2} \frac{\Sigma(q_E)}{\Sigma^2(q_E) + q_E^2}. \quad (7)$$

Here, an overall factor (the number of light quarks times the number of colors) is omitted and $m(\Lambda)$ is the bare quark mass. In the above equations we temporary introduced the ultraviolet cutoff Λ in order to make the bare quark mass well-defined.

The extremum condition for V with respect to $\Sigma(p_E)$ leads to the following SDE for the quark self-energy

$$\Sigma(p_E) = m(\Lambda) + 3C_2 \int^\Lambda \frac{d^4 q_E}{(2\pi)^4} \frac{\bar{g}^2(p_E, q_E)}{(p_E - q_E)^2} \frac{\Sigma(q_E)}{\Sigma^2(q_E) + q_E^2}. \quad (8)$$

In Higashijima–Miransky approximation, since the argument of the running coupling has no angle dependence, we first perform the angle integration. As a result, we understand that the procedure is achieved equivalently by replacing $(p_E - q_E)^{-2}$ by $\theta(p_E - q_E)(p_E^2)^{-1} + \theta(q_E - p_E)(q_E^2)^{-1}$ in Eq. (8). Then we can reduce Eq. (8) to the following differential equation [14]

$$\frac{\Sigma(p_E)}{\Sigma^2(p_E) + p_E^2} = \frac{(4\pi)^2}{3C_2} \frac{d}{p_E^2 dp_E^2} \left(\frac{1}{\Delta(p_E)} \frac{d\Sigma(p_E)}{dp_E^2} \right), \quad (9)$$

and the two boundary conditions

$$\left. \frac{1}{\Delta(p_E)} \frac{d\Sigma(p_E)}{dp_E^2} \right|_{p_E=0} = 0, \quad (10)$$

$$\Sigma(p_E) - \frac{\mathcal{D}(p_E)}{\Delta(p_E)} \frac{d\Sigma(p_E)}{dp_E^2} \Big|_{p_E=\Lambda} = m(\Lambda), \quad (11)$$

where the functions

$$\mathcal{D}(p_E) = \frac{\bar{g}^2(p_E)}{p_E^2} \quad (12)$$

and

$$\Delta(p_E) = \frac{d}{dp_E^2} \mathcal{D}(p_E), \quad (13)$$

are introduced.

Substituting Eqs. (8) and (9) into Eqs. (6) and (7), we obtain

$$\begin{aligned} V[\Sigma(p_E)] &= -2 \int^\Lambda \frac{d^4 p_E}{(2\pi)^4} \ln \frac{\Sigma^2(p_E) + p_E^2}{m^2(\Lambda) + p_E^2} \\ &\quad + 2 \int^\Lambda \frac{d^4 p_E}{(2\pi)^4} \frac{\Sigma(p_E)(\Sigma(p_E) - m(\Lambda))}{\Sigma^2(p_E) + p_E^2} \\ &= -2 \int^\Lambda \frac{d^4 p_E}{(2\pi)^4} \ln \frac{\Sigma^2(p_E) + p_E^2}{m^2(\Lambda) + p_E^2} \\ &\quad + \frac{2(4\pi)^2}{3C_2} \int^\Lambda \frac{d^4 p_E}{(2\pi)^4} [\Sigma(p_E) - m(\Lambda)] \frac{d}{dp_E^2} \left(\frac{1}{\Delta(p_E)} \frac{d\Sigma(p_E)}{dp_E^2} \right) \\ &= -2 \int^\Lambda \frac{d^4 p_E}{(2\pi)^4} \ln \frac{\Sigma^2(p_E) + p_E^2}{m^2(\Lambda) + p_E^2} \\ &\quad - \frac{2}{3C_2} \int^{\Lambda^2} dp_E^2 \frac{1}{\Delta(p_E)} \left(\frac{d}{dp_E^2} \Sigma(p_E) \right)^2 + V_S, \end{aligned} \quad (14)$$

where we used a partial integration in the last line and

$$\begin{aligned} V_S &= F(\Lambda) - F(0), \\ F(p_E) &= \frac{2}{3C_2} [\Sigma(p_E) - m(\Lambda)] \frac{1}{\Delta(p_E)} \frac{d\Sigma(p_E)}{dp_E^2}. \end{aligned} \quad (15)$$

Hereafter we consider the effective potential in the continuum limit ($\Lambda \rightarrow \infty$). Let us begin by evaluating $F(\Lambda)$ using the running coupling

$$\bar{g}^2(p_E) = \frac{2\pi^2 a}{\ln p_E^2}, \quad a \equiv \frac{24}{11N_c - 2n_f}, \quad (16)$$

and the corresponding asymptotic form of the mass function [19]

$$\Sigma(p_E) \rightarrow m(\Lambda) \left(\frac{\ln p_E^2}{\ln \Lambda^2} \right)^{-a/2} + \frac{\sigma}{p_E^2} (\ln p_E^2)^{a/2-1}, \quad (17)$$

where n_f is the number of flavors which controls the running coupling. Throughout this paper, we put $N_c = n_f = 3$, namely $a = 8/9$. The parameter σ is related to the order parameter of the chiral symmetry $\langle \bar{q}q \rangle$ as

$$\sigma = -\frac{2\pi^2 a \langle \bar{q}q \rangle}{3}. \quad (18)$$

When the chiral symmetry is exact, i.e., $m(\Lambda) = 0$, using Eqs. (16) and (17), we can easily show that $F(\Lambda)$ vanishes in the continuum limit, i.e., $\lim_{\Lambda \rightarrow \infty} F(\Lambda) = 0$. As for $F(0)$, since we introduce infrared finite running coupling and mass function in Eqs. (20) and (21), we can set $F(0) = 0$. After all, in the continuum limit, we get $V_S = 0$ and the modified version of the CJT effective potential is obtained as [15,20]

$$\begin{aligned} V[\Sigma(p_E)] &= -2 \int \frac{d^4 p_E}{(2\pi)^4} \ln \frac{\Sigma^2(p_E) + p_E^2}{p_E^2} \\ &\quad - \frac{2}{3C_2} \int dp_E^2 \frac{1}{\Delta(p_E)} \left(\frac{d}{dp_E^2} \Sigma(p_E) \right)^2. \end{aligned} \quad (19)$$

We can also show that $V_S = 0$, namely Eq. (19) holds for nonzero bare quark mass [21].

A few comments are in order.

(1) The extremum condition for Eq. (19) with respect to $\Sigma(p_E)$ leads to Eq. (9) which is equivalent to the original equation (8) in Higashijima–Miransky approximation apart from the two boundary conditions. We will take account of these conditions when we introduce the trial mass function.

(2) In the chiral limit, Eq. (19) is the same as the expression given in Refs. [15,20]. However, even if the chiral symmetry is explicitly broken, we can use the same expression for V [21]. We do not require the *finite renormalization* adopted in Ref. [15].

Now we are in a position to introduce a modified running coupling and a trial mass function. We use the following QCD-like running coupling [14]

$$\bar{g}^2(p_E) = \frac{2\pi^2 a}{\ln(p_E^2 + p_R^2)}, \quad (20)$$

where p_R is a parameter to regularize the divergence of the QCD running coupling at $p = 1(\Lambda_{\text{QCD}})$. This running coupling approximately develops according to the QCD renormalization group equation of one loop order, while it smoothly approaches a constant as p_E^2 decreases.

Hereafter we consider the chiral limit; i.e., the $m(\Lambda) = 0$ case. Corresponding to the QCD-like running coupling, the SDE with the two boundary conditions suggests the following trial mass function [14]

$$\Sigma(p_E) = \frac{\sigma}{p_E^2 + p_R^2} [\ln(p_E^2 + p_R^2)]^{a/2-1}, \quad (21)$$

where σ is the same as before.

Using Eqs. (20) and (21), we can express $V[\Sigma(p_E)]$ as a function of σ the order parameter. A further discussion of the CJT effective potential and the dynamical chiral symmetry breaking in QCD-like theory at zero temperature and density can be found in Refs. [14,15].

B. Effective potential at finite temperature and density

In this subsection we discuss the effective potential at finite temperature and density. In order to calculate the effective potential at finite temperature and density, we apply the imaginary time formalism [22]

$$\int \frac{dp_4}{2\pi} f(p_4) \rightarrow T \sum_{n=-\infty}^{\infty} f(\omega_n + i\mu), \quad (n \in \mathbf{Z}), \quad (22)$$

where $\omega_n = (2n + 1)\pi T$ is the fermion Matsubara frequency and μ represents the quark chemical potential. In addition, we need to define the running coupling and the (trial) mass function at finite T and/or μ . We adopt the following real functions for $\mathcal{D}_{T,\mu}(p)$ and $\Sigma_{T,\mu}(p)$

$$\mathcal{D}_{T,\mu}(p) = \frac{2\pi^2 a}{\ln(\omega_n^2 + \mathbf{p}^2 + p_R^2)} \frac{1}{\omega_n^2 + \mathbf{p}^2}, \quad (23)$$

$$\Sigma_{T,\mu}(p) = \frac{\sigma}{\omega_n^2 + \mathbf{p}^2 + p_R^2} [\ln(\omega_n^2 + \mathbf{p}^2 + p_R^2)]^{a/2-1}. \quad (24)$$

In Eq. (23) we do not introduce the μ dependence in $\mathcal{D}_{T,\mu}(p)$. The gluon momentum squared is the most natural argument of the running coupling at zero temperature and density, in the light of the chiral Ward–Takahashi identity [23]. Then it is reasonable to assume that $\mathcal{D}_{T,\mu}(p)$ does not depend on the quark chemical potential.

As concerns the mass function, we use the same function as Eq. (21) except that we replace p_4 with ω_n . As already noted in Sec. II A, the quark wave function does not suffer the renormalization in the Landau gauge for $T = \mu = 0$, while, the same does not hold for finite T and/or μ . However, we assume that the wave function renormalization is not required even at finite T and/or μ , for simplicity.

Furthermore, we neglect the T - μ dependent terms in the quark and gluon propagators which arise from the perturbative expansion. We expect that the phase structure is not so affected by these approximations.

Using Eqs. (23) and (24), it is easy to write down the effective potential at finite temperature and chemical potential (see Appendix). Assuming the mean-field expansion, the effective potential can be expanded as a power series in σ with finite coefficients $a_{2n}(T, \mu)$

$$V(\sigma; T, \mu) = a_2(T, \mu)\sigma^2 + a_4(T, \mu)\sigma^4 + \dots \quad (25)$$

Once we know the value of σ_{min} the location of the minimum of V , we can determine the value of $\langle \bar{q}q \rangle$ using the following relation

$$\langle \bar{q}q \rangle = -T \sum_n \int \frac{d^3 p}{(2\pi)^3} \text{Tr} S_{T, \mu}(p), \quad (26)$$

where $S_{T, \mu}(p)$ is the quark propagator at finite T and/or μ in our approximations and “Tr” refers to Dirac and color matrices. However, in this paper, we still determine the $\langle \bar{q}q \rangle$ through the relation $\langle \bar{q}q \rangle = -(3/2\pi^2 a)\sigma_{min}$. We have confirmed that this relation works well even at finite T and/or μ .

III. CHIRAL PHASE TRANSITION AT HIGH TEMPERATURE AND DENSITY

In our numerical calculation, as mentioned before, we put $N_c = n_f = 3$. Furthermore, since it was known that the quantities such as $\langle \bar{q}q \rangle$ and f_π are quite stable under the change of the infrared regularization parameter [10], we fix $t_R \equiv \ln(p_R^2/\Lambda_{\text{QCD}}^2)$ to 0.1 and determine the value of Λ_{QCD} by the condition $f_\pi = 93$ MeV at $T = \mu = 0$. We approximately reproduce f_π using the Pagels–Stoker formula [24]:

$$f_\pi^2 = 4N_c \int \frac{d^4 p_E}{(2\pi)^4} \frac{\Sigma(p_E)}{(\Sigma^2(p_E) + p_E^2)^2} \left(\Sigma(p_E) - \frac{p_E^2}{2} \frac{d\Sigma(p_E)}{dp_E^2} \right), \quad (27)$$

and obtain $\Lambda_{\text{QCD}} = 738$ MeV. The value of Λ_{QCD} is almost the same as the one obtained in the previous paper [12] in which we used Eqs. (6) and (7).

A. $T \neq 0, \mu = 0$ case

Fig. 2 shows the T -dependence of the effective potential at $\mu = 0$. We can realize that σ_{min} the minimum of the effective potential continuously goes to zero as temperature grows. Thus we have a second-order phase transition at $T_c = 129$ MeV. Fig. 3 shows the temperature dependence of $-\langle \bar{q}q \rangle^{1/3}$.

B. $T = 0, \mu \neq 0$ case

Fig. 4 shows the μ -dependence of the effective potential at $T = 0$. For small values of μ , the absolute minimum is nontrivial. However we find that the trivial and the nontrivial minima coexist at $\mu = 422$ MeV. For larger values of μ , the energetically favored minimum move to the origin. Thus we have a first-order phase transition at $\mu_c = 422$ MeV. Fig. 5 shows the chemical potential dependence of $-\langle \bar{q}q \rangle^{1/3}$. The chiral condensate vanishes discontinuously at $\mu = \mu_c$.

C. $T \neq 0, \mu \neq 0$ case

In the same way as the previous two cases, we determine the critical line on the T - μ plane (see Fig.6). The position of the tricritical point “ P ” is determined by the condition

$$a_2(T_P, \mu_P) = a_4(T_P, \mu_P) = 0, \quad (28)$$

in Eq. (25). Solving this equation, we have

$$(T_P, \mu_P) = (107, 210) \text{ MeV}.$$

We have varied t_R from 0.1 to 0.3 in order to examine the t_R dependence of the position of P . As a result, for instance, we have

$$\begin{aligned} (T_P, \mu_P) &= (104, 207) \text{ MeV} \quad \text{for } t_R = 0.2, \\ &= (101, 208) \text{ MeV} \quad \text{for } t_R = 0.3. \end{aligned}$$

We note that the value of Λ_{QCD} has been determined at $T = \mu = 0$ by the condition $f_\pi = 93$ MeV for each value of t_R . Thus we confirmed that the position of P is stable under the change of t_R .

IV. CONCLUSION

In this paper we studied the chiral phase transition at high temperature and/or density in the QCD-like theory.

We extended the effective potential to finite T and μ and studied the phase structure. We found the second-order phase transition at $T_c = 129$ MeV along the $\mu = 0$ line and the first-order phase transition at $\mu_c = 422$ MeV along the $T = 0$ line. We also studied the phase diagram and found a tricritical point P at $(T_P, \mu_P) = (107, 210)$ MeV. Phase diagrams with similar structure have been obtained in other QCD-like theories [9,13]. As concerns the position of the tricritical point, however, our result is not close to theirs. Let us consider the reason why our model gives the different result. In Ref. [9], they used the momentum independent coupling and the mass function without logarithmic behavior. The values of T_c and μ_c of Ref. [13] are about the same as ours. However, the position of the tricritical point is in the region of small μ . The discrepancy may arise from the fact that: (1) They did not use the variational method, but numerically solved the SDE; (2) The treatment of the gluon propagator at finite T and/or μ is different from ours. Our result is rather consistent with that of the NJL model [2] and the random matrix model [3]. They obtained

$$T_P \sim 100 \text{ MeV} \quad , \quad 3\mu_P \sim (600 - 700) \text{ MeV}.$$

Recently it was pointed out that the values of T and μ accomplished in high-energy heavy-ion collisions may be close to the tricritical point and it may be possible to observe some signals [1]. Thus it is significant that three different models show almost the same results.

Finally, some comments are in order. In this paper, we modified the form of the CJT effective potential at $T = \mu = 0$ using the two representation of the SDE. Our formulation of the effective potential is entirely based on the Higashijima–Miransky approximation. It was known that the approximation breaks the chiral Ward–Takahashi identity. Therefore, it is preferable to formulate the effective potential without this approximation. However it seems that the results do not depend on choice of the argument momentum [23,25]. Moreover, the treatment of the quark and the gluon propagators at finite T and/or μ is somewhat oversimplified in the present work. We would like to consider the wave function renormalization and more appropriate functional form for $\mathcal{D}_{T,\mu}(p)$ and $\Sigma_{T,\mu}(p)$. By including a finite quark mass, we can study a more realistic situation where the chiral symmetry is explicitly broken. In the studies of SDE with the finite quark mass, it was known that there is a difficulty in removing a perturbative contribution from the quark condensate [19,26]. In the effective potential approach, however, we are free from such a difficulty. The study of the phase structure with the finite quark mass is now in progress [21]. Furthermore, we also plan to study the quark pairing including a color superconductivity [2,4–8] and a “color-flavor locking” [7] (for $N_c = N_f = 3$ case), in the QCD-like theory.

APPENDIX:

In this appendix, we show the effective potential explicitly. In the first place, we consider the case of zero temperature and finite chemical potential.

Using Eq. (24), we obtain

$$\begin{aligned} V_1 &= -2 \int \frac{d^4 p_E}{(2\pi)^4} \ln \frac{\Sigma_{T,\mu}^2(p) + (p_4 + i\mu)^2 + \mathbf{p}^2}{(p_4 + i\mu)^2 + \mathbf{p}^2} \\ &= -\frac{1}{4\pi^3} \int_p \ln \left[\frac{(\Sigma_{T,\mu}^2(p) + p_4^2 + \mathbf{p}^2 - \mu^2)^2 + (2\mu p_4)^2}{(p_4^2 + \mathbf{p}^2 - \mu^2)^2 + (2\mu p_4)^2} \right], \end{aligned} \quad (\text{A1})$$

where the imaginary part of V_1 is odd function of p_4 ; therefore it has been removed from Eq. (A1) and

$$\int_p = \int_{-\infty}^{\infty} dp_4 \int_0^{\infty} d|\mathbf{p}| \mathbf{p}^2. \quad (\text{A2})$$

In Eq. (19), we carry out the momentum-differentiation and, then, use Eqs. (23) and (24). V_2 is obtained as

$$\begin{aligned} V_2 &= \frac{4\sigma^2}{3\pi^3 C_2 a} \int_p \frac{(p_4^2 + \mathbf{p}^2)^2 [\ln(p_4^2 + \mathbf{p}^2 + p_R^2)]^{a-2}}{(p_4^2 + \mathbf{p}^2 + p_R^2) \ln(p_4^2 + \mathbf{p}^2 + p_R^2) + p_4^2 + \mathbf{p}^2} \\ &\quad \times \frac{1}{(p_4^2 + \mathbf{p}^2 + p_R^2)^3} \left[\ln(p_4^2 + \mathbf{p}^2 + p_R^2) + 1 - \frac{a}{2} \right]^2. \end{aligned} \quad (\text{A3})$$

At finite temperature and chemical potential, the p_4 integration in Eqs. (A1) and (A3) is replaced by the sum over the Matsubara frequencies.

- [1] M. Stephanov, K. Rajagopal and E. Shuryak, Phys. Rev. Lett. **81**, 4816 (1998).
- [2] J. Berges and K. Rajagopal, Nucl. Phys. B **538**, 215 (1999).
- [3] M. A. Halasz, A. D. Jackson, R. E. Shrock, M. A. Stephanov and J. J. M. Verbaarschot, Phys. Rev. D **58**, 096007 (1998).
- [4] D. Bailin and A. Love, Phys. Rep. **107**, 325 (1984).
- [5] M. Iwasaki and T. Iwado, Phys. Lett. B **350**, 163 (1995).
- [6] T. Schäfer and F. Wilczek, Phys. Rev. D **60**, 114033 (1999); R. D. Pisarski and D. H. Rischke, nucl-th/9907041; nucl-th/9910056; D. K. Hong, V. A. Miransky, I. A. Shovkovy and L. C. R. Wijewardhana, Phys. Rev. D **61**, 056001 (2000); W. E. Brown, J. T. Liu and H. -C. Ren, hep-ph/9908248; D. H. Hsu and M. Schwetz, hep-ph/9908310.
- [7] M. Alford, K. Rajagopal and F. Wilczek, Nucl. Phys. B **537**, 443 (1999); T. Schäfer, hep-ph/9909574; I. Shovkovy and L. C. R. Wijewardhana, Phys. Lett. B **470**, 189 (1999).
- [8] For reviews of conjectured QCD phase diagrams including both the chiral condensate and the color superconducting condensate, see, M. Alford, hep-lat/9809166; K. Rajagopal, hep-ph/9908360.
- [9] A. Barducci, R. Casalbuoni, S. De Curtis, R. Gatto and G. Pettini, Phys. Rev. D **41**, 1610 (1990).
- [10] Y. Taniguchi and Y. Yoshida, Phys. Rev. D **55**, 2283 (1997).
- [11] D. Blaschke, C. D. Roberts and S. Schmidt, Phys. Lett. B **425**, 232 (1998); C. D. Roberts and S. Schmidt, nucl-th/9903075.
- [12] O. Kiriya, M. Maruyama and F. Takagi, Phys. Rev. D **58**, 116001 (1998).
- [13] M. Harada and A. Shibata, Phys. Rev. D **59**, 014010 (1998).
- [14] K. Higashijima, Prog. Theor. Phys. Suppl. **104**, 1 (1991).
- [15] A. Barducci, R. Casalbuoni, S. De Curtis, D. Dominic and R. Gatto, Phys. Rev. D **38**, 238 (1988).
- [16] J. M. Cornwall, R. Jackiw and E. Tomboulis, Phys. Rev. D **10**, 2428 (1974).
- [17] K. Higashijima, Phys. Lett. B **124**, 257 (1983).
- [18] V. A. Miransky, Sov. J. Nucl. Phys. **38**, 280 (1984).
- [19] See, for example,
V. A. Miransky, *Dynamical Symmetry Breaking in Quantum Field Theories* (World Scientific, Singapore, 1993).
- [20] J. C. Montero and V. Pleitez, Z. Phys. C **50**, 149 (1991).
- [21] O. Kiriya, M. Maruyama and F. Takagi, in preparation.
- [22] See, for example,
J. I. Kapusta, *Finite temperature field theory* (Cambridge University Press, Cambridge, England, 1989).
- [23] T. Kugo and M. G. Mitchard, Phys. Lett. B **282**, 162 (1992); *ibid.* **286**, 355 (1992).
- [24] H. Pagels and S. Stoker, Phys. Rev. D **20**, 2947 (1979).
- [25] K-I. Aoki, M. Bando, T. Kugo, M. G. Mitchard and H. Nakatani, Prog. Theor. Phys. **84**, 683 (1990); K-I. Aoki, M. Bando, T. Kugo and M. G. Mitchard, *ibid.* **85**, 355 (1991).
- [26] K. Kusaka, H. Toki and S. Umisedo, Phys. Rev. D **59**, 116010 (1999).

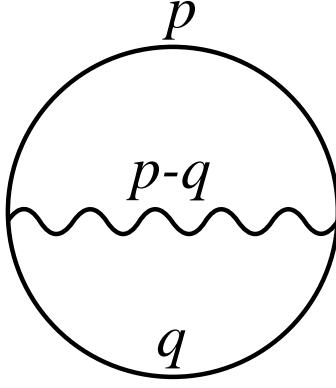


FIG. 1. Two-particle irreducible graph which contributes to V_2 .

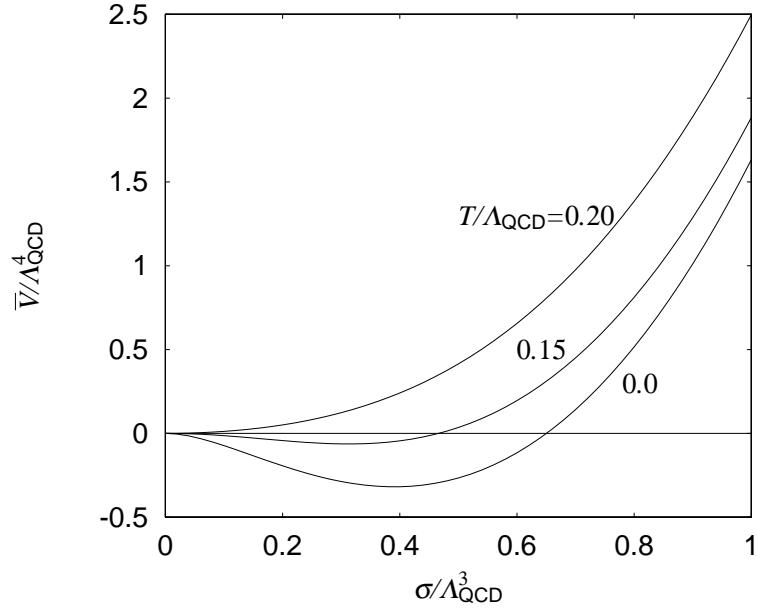


FIG. 2. The effective potential at finite temperature and zero chemical potential. \bar{V} is defined by $\bar{V} = 24\pi^3 V$ and all quantities are taken to be dimensionless. The curves show the cases $T/\Lambda_{\text{QCD}} = 0, 0.15, 0.2$.

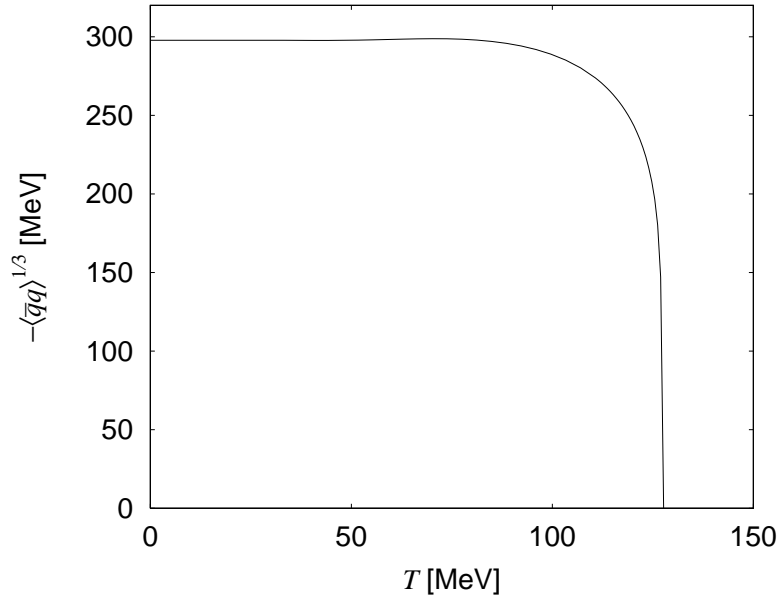


FIG. 3. The temperature dependence of $-\langle\bar{q}q\rangle^{1/3}$ at $\mu = 0$.

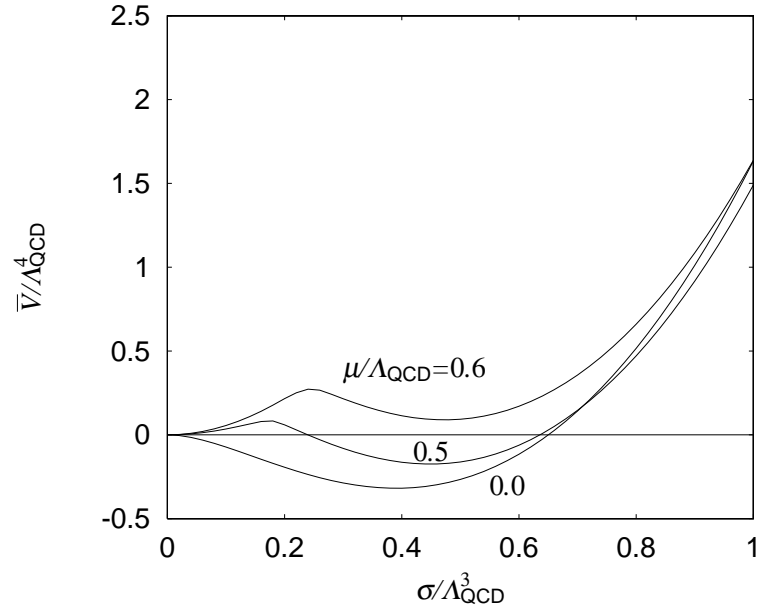


FIG. 4. The effective potential at finite chemical potential and zero temperature. The curves show the cases $\mu/\Lambda_{\text{QCD}} = 0, 0.5, 0.6$.

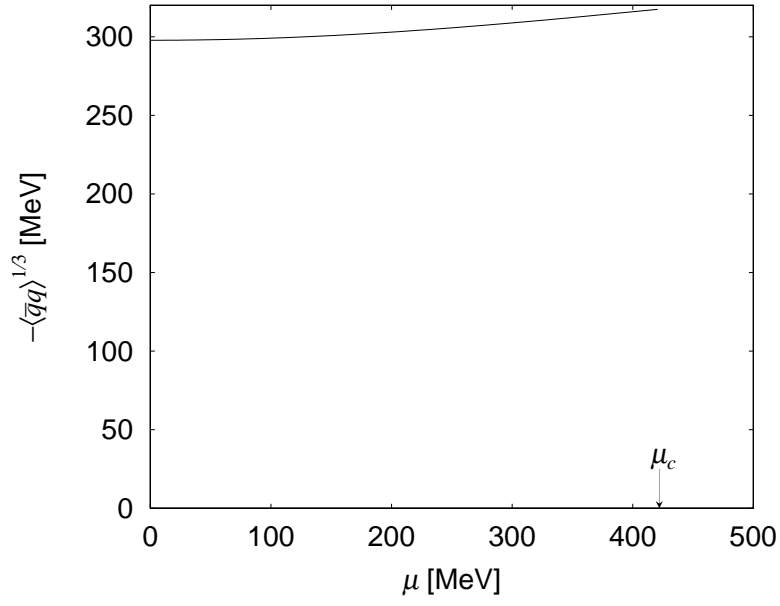


FIG. 5. The chemical potential dependence of $-\langle\bar{q}q\rangle^{1/3}$ at $T = 0$.

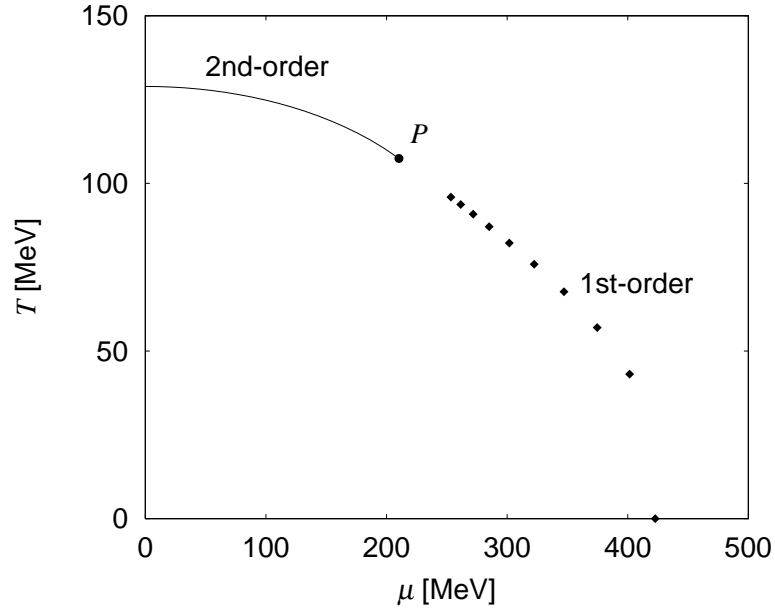


FIG. 6. The phase diagram in the T - μ plane. Solid line indicates the phase transition of second-order and points indicate that of first-order. The point P is the tricritical point.